White Matter Governed Superior Frontal Sulcus Surgical Paradigm: A Radioanatomic Microsurgical Study—Part II

Amin B. Kassam, MD[*‡]
Alejandro Monroy-Sosa, MD[*]
Melanie B. Fukui, MD[*]
Bhavani Kura, MD[*]
Jonathan E. Jennings, MD[*]
Juanita M. Celix, MD, MPH[*]
Kenneth C. Nash, MD[§]
Mikaeel Kassam[*‡]
Richard A. Rovin, MD[*]
Srikant S. Chakravarthi, MD, MSc[*]

[*]Department of Neurosurgery, Aurora Neuroscience Innovation Institute, Aurora St. Luke's Medical Center, Milwaukee, Wisconsin; [‡]Neeka Health, Milwaukee, Wisconsin; [§]Department of Psychiatry, University of Pittsburgh Medical Center, Pittsburgh, Pennsylvania

Correspondence:
Amin B. Kassam, MD,
Aurora St. Luke's Medical Center,
Suite 630,
2801 W Kinnickinnic River Pkwy,
Milwaukee, WI 53215, USA.
Email: amin.kassam@aurora.org

Received, April 25, 2019.
Accepted, February 2, 2020.

BACKGROUND: Kocher's point (KP) and its variations have provided standard access to the frontal horn (FH) for over a century. Anatomic understanding of white matter tracts (WMTs) has evolved, now positioning us to better inform the optimal FH trajectory.

OBJECTIVE: To (1) undertake a literature review analyzing entry points (EPs) to the FH; (2) introduce a purpose-built WMT-founded superior frontal sulcus parafascicular (SFSP)-EP also referred to as the Kassam-Monroy entry point (KM-EP); and (3) compare KM-EP with KP and variants with respect to WMTs.

METHODS: (1) Literature review (PubMed database, 1892-2018): (a) stratification based on the corridor: i. ventricular catheter; ii. through-channel endoscopic; or iii. portal; (b) substratification based on intent: i. preoperatively planned or ii. intraoperative (postdural opening) for urgent ventricular drainage. (2) Anatomic comparisons of KM-EP, KP, and variants via (a) cadaveric dissections and (b) magnetic resonance-diffusion tensor imaging computational 3D modeling.

RESULTS: A total of 31 studies met inclusion criteria: (a) 9 utilized KP coordinate (1 cm anterior to the coronal suture (y-axis) and 3 cm lateral of the midline (x-axis) approximated by the midpupillary line) and 22 EPs represented variations. All 31 traversed critical subcortical WMTs, specifically the frontal aslant tract, superior longitudinal fasciculus II, and inferior fronto-occipital fasciculus, whereas KM-EP ($x = 2.3$, $y = 3.5$) spares these WMTs.

CONCLUSION: KP ($x = 3$, $y = 1$) conceived over a century ago, prior to awareness of WMTs, as well as its variants, anatomically place critical WMTs at risk. The KM-EP ($x = 2.3$, $y = 3.5$) is purpose built and founded on WMTs, representing anatomically safe access to the FH. Correlative clinical safety, which will be directly proportional to the size of the corridor, is yet to be established in prospective studies.

KEY WORDS: Kocher's point, Frontal horn, Lateral ventricle, Superior frontal sulcus (SFS), Parafascicular, Catheter, Endoscope, Port, Subcortical frontal lobe, Ventricular catheter

Operative Neurosurgery 0:1–13, 2020 DOI: 10.1093/ons/opaa066

Accessing the frontal horn of the lateral ventricle is one of the most common procedures in neurosurgery. Emil Theodor Kocher in 1892[1] utilized a craniometer to describe surface osseous coordinates to consistently access the frontal horn; this has been the standard entry point (EP) for over a century. Over the ensuing century, several variations have emerged, which have also relied upon osseous, vasculature, and, subsequently, cortical (motor cortex) considerations; notably, the subcortical white matter tracts (WMTs) have not, to date, been a defining consideration.[2-14]

Over time, Kocher's point (KP) has provided access not only to the frontal horn, but also to the subcortical region. In addition,

ABBREVIATIONS: CASN, computer-assisted stereotactic navigation; **CCF,** claustrocortical fiber; **CS,** coronal suture; **DTI,** diffusion tensor imaging; **EP,** entry point; **FAT,** frontal aslant tract; **FH,** frontal horn; **IFOF,** inferior fronto-occipital fasciculus; **KM-EP,** Kassam-Monroy entry point; **KP,** Kocher's point; **MR,** magnetic resonance; **SFS,** superior frontal sulcus; **SFS-DD,** SFS-distal division; **SFS-MD,** SFS-middle division; **SFSP,** SFS parafascicular; **SFSP-EP,** SFS parafascicular entry point; **SFS-PD,** SFS-proximal division; **SLF-II,** superior longitudinal fasciculus II; **SLF-III,** superior longitudinal fasciculus III; **SSS,** superior sagittal sinus; **3D,** 3-dimensional; **WMT,** white matter tracts

endoscopic approaches to ventricular pathology, eg, colloid cysts, have utilized KP or its variations via through-channel endoscopy or tubular retractors.[10,15-17] Although the impact on WMTs may be minimal, in the case of 2-mm ventricular catheters, as diameters of the tubular retractor have progressively increased (up to 20 mm), the effect may be proportionally greater.

Recent advancement of magnetic resonance-diffusion tensor imaging (MR-DTI), along with enhanced knowledge of WMT organization, has led to functional awareness of neurocognitive pathways and their anatomic substrates.[18,19] These subcortical networks now play a critical role in redefining initial osseous and cortical-based EPs, particularly for larger diameter access. As imaging and understanding of the vital function of subcortical anatomy has evolved, we now have opportunity to refine the original frontal horn trajectory defined over a century ago.

Recently, multiple authors have forwarded transsulcal parafascicular corridor surgery to access subcortical, periventricular, and ventricular pathologies,[20-26] with the ideological goal of minimizing the impact on neural tissue.[18,19] Although beyond the scope of this report, in an accompanying report, we have detailed a schema organizing key subcortical WMTs surrounding the superior frontal sulcus (SFS) into medial, intervening, and lateral segments, creating a reproducible anatomic corridor optimizing preservation of WMTs.

Objectives

1. Provide a literature review of current EPs to the frontal horn and subcortical frontal lobe.
2. Provide cadaveric subcortical dissections facilitating qualitative comparison of KP and its major variations in the context of WMTs traversed.
3. Introduce a purpose-built WMT-founded SFS parafascicular entry point (SFSP-EP), also referred to as the Kassam-Monroy entry point (KM-EP).
4. Provide DTI-guided 3-dimensional (3D) renderings comparing KP and KM-EP.

METHODS

Literature Review

The literature search (PubMed database, 1892-2018) included the following keywords: "Kocher's point," "frontal horn," "periventricular region," "third ventricle," "colloid cyst," "subcortical frontal lesion," and "ventricular entry point." Only articles detailing EP anatomic landmarks were included; specifically, only studies whose primary objective was to provide anatomic descriptions, as opposed to clinical outcomes, were considered, representing a qualitative literature search. Duplicate studies were excluded. Absence of primary outcome measures precluded quantitative analysis.

Stratification occurred based on the corridor: (a) ventricular catheter, ie, external or indwelling, (b) through-channel endoscopy, or (c) tubular retractor. Catheter subgroup was further substratified based on intent: (a) preoperatively planned or (b) intraoperative (postdural opening) urgent ventricular drainage. Additional substratification based on cannulation technique (ie, freehand or image-guided computer-assisted-stereotactic navigation [CASN] or ultrasound) was undertaken.

Neuroanatomical Study

Ten embalmed cadaveric specimens injected with red-blue silicon were frozen (2 wk at −15°C) and prepared as previously described.[27,28] Osseous landmarks (ie, superior parietal line, coronal suture (CS), frontal projection of the superior sagittal sinus (SSS), and the middle part of the orbital crest corresponding to midpupillary line) were analyzed relative to the divisions of the SFS and underlying WMT segments consistent with the accompanying schema (see below). Distance from osseous landmarks to EPs was measured using digital calipers (Vernier Software & Technology, Beaverton, Oregon). Catheters were used to simulate EP frontal horn trajectories including our purpose-built trajectory. Through panoramic photographs, KP, variations, and the SFSP-EP were illustrated with the respective key WMTs at "anatomic risk." Neuronavigation was used to correlate the SFSP-EP with external landmarks, with the intent to create surface landmarks in the event that CASN is not available.

Radiological Study

DTI-MRI tractography models were rendered, comparing KP to the purpose-built SFSP-EP, demonstrating the anatomic impact on the WMTs.

Institutional Review Board approval was not required for any portion of this study, as patient information was not retrieved or utilized (non-Human Subject Determination).

RESULTS

Literature Review

Intent-Based Stratification

Preoperatively planned: substratification of the 39 EPs to frontal horn based on technique yielded ultrasound and navigation (N = 1),[29] CASN (N = 13),[8,17,30-38] and freehand (N = 25) (Table 1).[1,4,7,9,15,39-58]

Intraoperative cannulation: separate and distinct from the 39 studies reporting preoperative planned coordinates; 5 additional reports described postdural opening access coordinates to the frontal horn.[3,5,6,11,59] Table 2 summarizes these intraoperative EPs and their respective anatomically "at risk" WMTs.

Corridor-Based Stratification

The 39 studies were stratified based on corridor: (a) 15 ventricular catheter (4 mm),[1,4,15,31,35,39-41,47,52,53,56-58] (b) 18 through-channel endoscopy (9 mm),[7-9,17,34,37(p),43-47,49-52,55-56] and (c) 6 tubular retractor (9-20 mm).[20,30,32,33,36,38] Seven used KP,[1,29,32,39,48,56,57] and 32 used variant EPs (Table 1).[4,7-9,15,17,20,30,31,33-38,40-47,49-55,58,60]

Anatomic Comparisons

Although beyond the scope of this paper, however, prior to comparing KP, variants, and the purpose-built KM-EP, there needs to be a detailed understanding of the frontal subcortical WMT framework. We have documented this in an accompanying anatomically based paper; however, for the convenience of the

TABLE 1. Historical Literature Review of Ventricular Access Points

	Authors	Technique	Corridor	Coronal plane lateral to midline	Sagittal/AP plane coronal suture	Major WMT(s) at risk
1	Kocher (1892)[1]	Freehand	VC	2.5 to 3 cm	1 cm	SLF II, FAT
2	Tillmanns (1908)[39]	Freehand	VC	3 cm	1 cm	SLF II, FAT
3	Kaufmann and Clark (1970)[4]	Freehand	VC	3 cm	4 cm above nasion	IFOF, UF
4	Madrazo Navarro et al (1981)[40]	Freehand	VC	Rostral third of the roof of the orbit	3 cm	FAT
5	Ghajar (1985)[41]	Freehand	VC	3 cm	10 cm above nasion	SLF II, FAT
6	Lewis et al (1994)[9]	Freehand	TCE	5 cm	1 cm ant. to CS	FAT SLF II, SLF III
7	Cabbell and Ross (1996)[30]	CASN	TPR	Middle frontal gyrus	Ant. to CS	FAT, SLF II
8	Abdou and Cohen (1998)[7]	Freehand	TCE	MPL	Ant. to CS	SLF II, FAT
9	Decq et al (1998)[42]	Freehand	TCE	3 cm	10 cm above superior orbital arch	SLF II IFOF
10	King et al (1999)[43]	Freehand	TCE	5 cm	1 cm ant. to CS	FAT SLF II, SLF III
11	Teo (1999)[44]	Freehand	TCE	5 to 6 cm	11 cm behind to nasion	SLF II, SLF III, IFOF
12	Longatti et al (2000)[45]	Freehand	TCE	2 to 5 cm	1 to 4 cm ant. to CS	SLF II, SLF III, IFOF, FAT
13	Rodziewicz et al (2000)[46]	Freehand	TCE	3 to 5 cm	2 cm ant. to CS	SLF II, SLF III, IFOF, FAT
14	O'Leary et al (2000)[47]	Freehand	VC	3 cm	10 cm above nasion	SLF II, FAT
15	Krotz et al (2004)[31]	CASN	VC	2 to 3 cm	11 cm above nasion	SLF II, FAT
16	Zohdi and El Kheshin (2006)[48]	Freehand	TCE	3 cm	Precoronal Kocher's point	SLF II, FAT
17	Acerbi et al (2007)[49]	Freehand	TCE	3 cm	11 above nasion	SLF II, FAT
18	Levine et al (2007)[50]	Freehand	TCE	5 cm	1 cm ant. to CS	SLF II, SLF III, IFOF, FAT
19	Greenlee et al (2008)[51]	Freehand	TCE	7 cm	8 cm above nasion	SLF II, SLF III, IFOF, FAT
20	Harris et al (2008)[32]	CASN	TPR	2 to 4 cm	1 cm ant. to CS	SLF II, FAT
21	Kakarla et al (2008)[52]	Freehand	VC	3 cm lateral to MPL	10 cm above nasion	SLF II, FAT
22	Ehtisham et al (2009)[53]	Freehand	VC	3 cm lateral to MPL	11-12 cm above nasion	SLF II, FAT
23	Mishra et al (2010)[54]	Freehand	TCE	4 to 5 cm	4 cm ant. to CS	SLF II, SLF III IFOF
24	Engh et al (2010)[33]	CASN	TPR	2.5 cm	CS	SLF II, FAT
25	Boogaarts et al (2011)[55]	Freehand	TCE	4 to 5 cm	1 cm ant. to CS	SLF II, SLF III, IFOF, FAT
26	Delitala et al (2011)[34]	CASN	TCE	MPL	1.5 cm above orbital rim	IFOF, UF
27	Hsieh et al (2011)[56]	Freehand	VC	2.5 cm	1	SLF II, SLF III, IFOF, FAT
28	Yamada et al (2012)[57]	Freehand	VC	1.5 to 3.5 cm	2.0	SLF II, SLF III, IFOF, FAT
29	Abdoh et al (2012)[58]	Freehand	VC	MPL	10 cm above supraorbital ridge	SLF II, IFOF
30	Thomale et al (2013)[35]	CASN	VC	1.75 cm	1.19 cm (above nasion)	IFOF, UF
31	Rehman et al (2013)[15]	Freehand	VC	3 cm	10 (above nasion)	SLF II, IFOF
32	Wilson et al (2013)[16]	CASN	TCE	5 to 7 cm	5 cm	SLF II, SLF III, IFOF
33	Cohen-Gadol (2013)[36]	CASN	TPR	–	Ant. to the CS	SLF II, FAT
34	McLaughlin et al (2013)[20]	CASN	TPR	SFS-PD	Ant. to the CS	SLF II, FAT
35	Rangel-Castilla et al (2014)[37]	CASN	TCE	4 cm	4.5 cm ant. to CS	SLF III, SLF II IFOF
36	Jakola et al (2014)[29]	US and CASN	VC	3 cm	1 cm ant. to CS	SLF II, FAT

TABLE 1. Continued

	Authors	Technique	Corridor	Coronal plane lateral to midline	Sagittal/AP plane coronal suture	Major WMT(s) at risk
37	Nasi et al (2017)[8]	CASN	TCE	MPL	2.5 to 3 cm above the eyebrow	IFOF, SLF II
38	Aref et al (2017)[60]	CASN	TCE	9 cm above pupil at MPL	4 cm ant. to CS (3 cm ant. to KP)	SLF II, IFOF
39	Eichberg et al (2018)[38]	CASN	TPR	SFS-DD	5 cm anterior to Kocher's point	Corona radiata
	Our study, 2019	CASN	Port	2.3 cm	3.5 cm	No major tracts involved, minor tracts: forceps minor

AP = anterior-posterior, WMT = white matter tract, CASN = computer-assisted stereotactic navigation; VC = ventricular catheter; MPL = midpupillary line; SFS = superior frontal sulcus; PD = proximal division; DD = distal division; CS = coronal suture; KP = Kocher's point; SLF II = superior longitudinal fasciculus II; FAT = frontal aslant tract; IFOF = inferofrontal occipital fasciculus; UF = uncinate fasciculus; SLF III = superior longitudinal fasciculus III.

TABLE 2. Intraoperative Urgent Cannulation Points

	Authors	Coronal/lateral plane (x-axis)	Sagittal/AP plane (y-axis)	Major WMT(s) at risk
1	Paine et al (1988)[6]	2.5 cm anterior to Sylvian fissure	2.5 cm superior to orbital surface of frontal lobe	SLF II, SLF III, IFOF, FAT
2	Hyun et al (2007)[3]	2.0 cm anterior to Paine x-axis (anterior limb extension)		SLF II, SLF III, IFOF, FAT
3	Park and Hamm (2007)[11]	4.5 cm anterior to Sylvian fissure	2.5 cm superior to lateral orbital roof	SLF II, SLF III, IFOF, FAT
4	Menovsky et al (2006)[5]	*Supraorbital burr hole*		UF, IFOF
		45° toward midline	20° up and parallel to orbitomeatal line	
5	Kim and Kang (2019)[59]	Middle frontal gyrus along incision line of dura mater		SLF II, SLF III

AP = anterior-posterior, WMT = white matter tract, SLF II = superior longitudinal fasciculus II, SLF III = superior longitudinal fasciculus III, IFOF = inferofronto occipital fasciculus, FAT = frontal aslant tract, UF = uncinate fasciculus.

reader, and to provide context for comparisons of EPs, we provide key considerations below.

Topographic Anatomy of the SFS–Complex

(a) Osseous: CS is the fiduciary bony landmark defining the origin of the SFS-middle division (MD). In the sagittal plane/anterior-posterior (y-axis), the most important tract directly below SFS is frontal aslant tract (FAT). Although FAT is located posterior to CS under SFS-proximal division (PD), imperatively, note that the distal end of FAT extends on average 1.96 cm anterior to CS, thereby extending into SFS-MD.

By corollary, in the coronal plane/lateral (x-axis), superior longitudinal fasciculus II (SLF-II) is the most critical WMT surrounding the SFS, located based on our schema in the lateral segment (see below), ie, lateral to the SFS and in between it and IFS. With respect to osseous landmarks, the SLF-II is located 3 cm lateral to SSS with the midpupillary line, representing an external landmark to locate SLF-II; note Kocher's x-coordinate (y = 1, x = 3) is at midpupillary line, whereas SFS is located on average 2.37 cm lateral to SSS, placing it medial to SLF-II. Alternatively, SFS can be identified medial to the superior temporal line at an average distance of 3.0 cm (Figure 1).

(b) Vasculature: relevant arteries are the prefrontal artery (branch of the middle cerebral artery) and the middle internal frontal artery (branch of the anterior cerebral artery). The middle frontal vein is the primary regional vein.

(c) Cortical gyri consists of superior frontal, middle frontal, and precentral gyri.

(d) Sulcus: SFS separating superior frontal gyrus from middle frontal gyrus.

The SFS complex is divided into 3 divisions (Figure 1):

(i) SFS-PD extends from the precentral sulcus to CS.
(ii) SFS-MD originates at CS extending 3.0 cm anteriorly.
(iii) SFS-distal division (SFS-DD) originates at the most distal portion of SFS-MD, extending 5.5 cm anteriorly, terminating at the orbital crest.

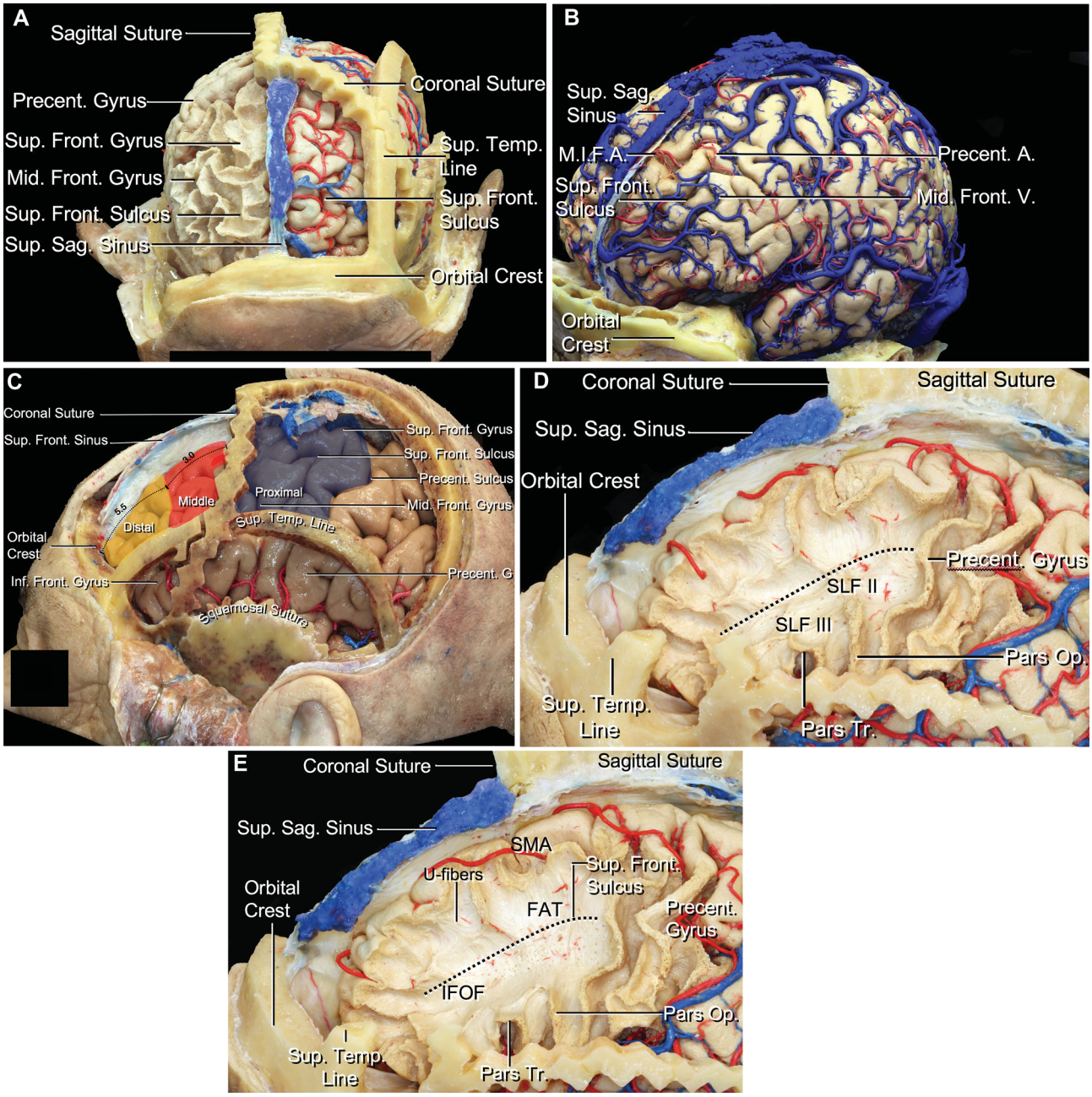

(FIGURE 1. *Cortical and subcortical anatomy of the superior frontal sulcus (SFS) region.* **A**, *Anterior-superior view of the frontal lobe. The relevant osseous landmarks of the frontal bone are showed in relation to the SFS. Subcortical and cortical anatomy are shown on the left and right sides, respectively.* **B**, *Vasculature of the lateral surface of the brain is shown here.* **C**, *The SFS complex is divided in 3 divisions: (1) SFS-PD, (2) SFS-MD, and (3) SFS-DD.* **D**, *Subcortical anatomy of the SFS complex. The cortex of the frontal lobe was removed.* **E**, *SLF-II and SLF-III were removed, and the frontal aslant tract (FAT) and the inferior fronto-occipital fasciculus (IFOF) were revealed. Front. = frontal; Inf. = inferior; Mid. = middle; M.I.F.A. = middle internal frontal artery; Op. = opercularis; Precent. = precentral; Pre. Fr. A. = prefrontal artery; Sag. = sagittal; SLF = superior longitudinal fascicle; SMA = supplementary area; Sup. = superior; Temp. = temporal; Tr. = triangularis; V. = vein.*

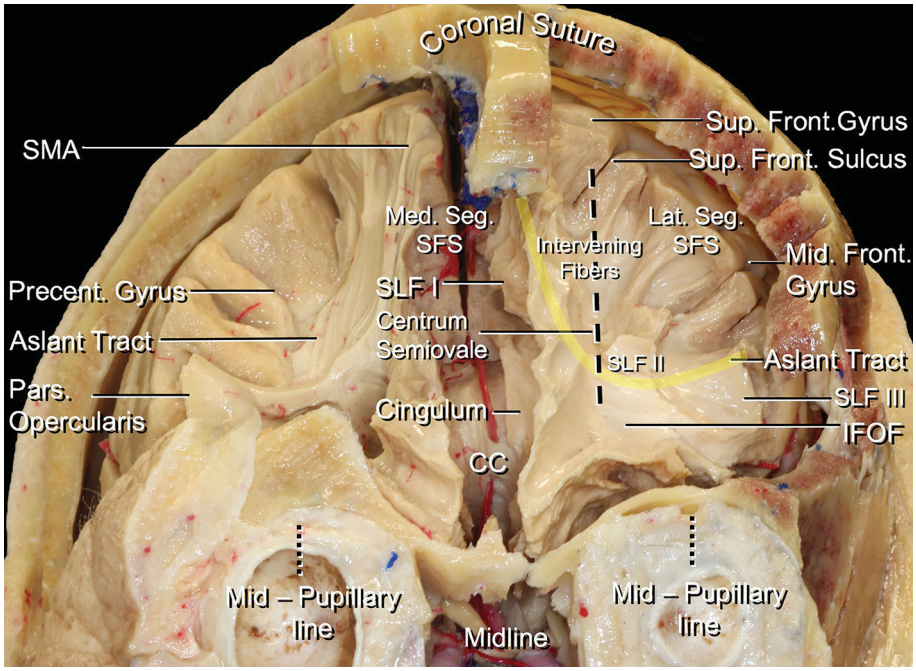

FIGURE 2. *Coronal view of the subcortical anatomy of the superior frontal sulcus (SFS) complex. The medial segment of the SFS complex is formed by the FAT, SLF-I, and the cingulum. The intervening segment is mainly formed by the corona radiata. The lateral segment of the SFS complex comprises of SLF-II, FAT, and IFOF. CC = corpus callosum; Front. = frontal; IFOF = inferior fronto-occipital fasciculus; Mid. = middle; Precent. = precentral; Seg. = segment; SLF. = superior longitudinal fasciculus; SMA = supplementary area.*

(e) WMTs: we grouped WMTs into regional segments juxtaposed around the SFS: (1) underlying middle frontal gyrus (lateral segment: U fibers, SLF-II, FAT, and inferior fronto-occipital fasciculus [IFOF]); (2) immediately below SFS (intervening segment: corona radiata); and (3) underlying superior frontal gyrus (medial segment: FAT, SLF-I, and cingulum). To avoid confusion, note that SFS topography is divided into divisions, and WMTs below SFS are compartmentalized into segments; medial segment refers to the WMT organization juxtaposed beneath the SFS, whereas the MD refers to the topography of SFS representing the division between the SFS-PD and SFS-DD (Figure 2).

Optimal Anatomic Subcortical Window

Cadaveric and 3D radiological data, based on the position of FAT, demonstrated the ideal EP in the y-axis (sagittal/anterior-posterior plane) must by definition be greater than 3.5 cm anterior to CS; analogously, based on the location of SLF-II, the x-axis (coronal/lateral plane) must be less than 3 cm. This SFSP-EP ($x = 2.3$, $y \geq 3.5$) is along the distal segment of the SFS and is more anterior and angled more acutely (in relation to the level of the SSS) than KP; thus, the traditional tragus landmark for the y-axis does not apply, rather, based on anatomic dissections and navigation; we found the mastoid tip as an accurate landmark in the y-axis or sagittal plane. In the coronal plane (x-axis), we found the medial canthus, similar to KP, as a suitable external landmark. With these external landmarks and the relative angle and trajectory of the SFSP-EP, an external ventricular catheter can be placed, without CASN, according to the anatomic principles outlined in the manuscript (see below) (Figures 3 and 4).

Comparisons of KP and Reported Variations

Although KP and all reported variant EPs provide consistent access to the frontal horn, each to varying degrees, including KP, place multiple major WMTs at "anatomic risk." Tables 1 and 2 and Figure 5 document and illustrate the coordinates of KP, variations, and the purpose-built SFSP-EP in the context of WMTs, respectively, at "anatomic risk." Variations were divided into 2 broad considerations: (a) lateral to KP in the coronal plane ($x \geq 3$ cm) and (b) adjacent to KP in the sagittal plane ($y \leq 1$ cm). Explicitly, EPs located 3 cm (or greater) lateral to SSS increasingly place the WMTs in the lateral (SLF-II/III and IFOF) and intervening (corona radiata, claustrocortical fiber [CCF], and FAT) SFS segments at anatomic risk. All EPs located in the sagittal or

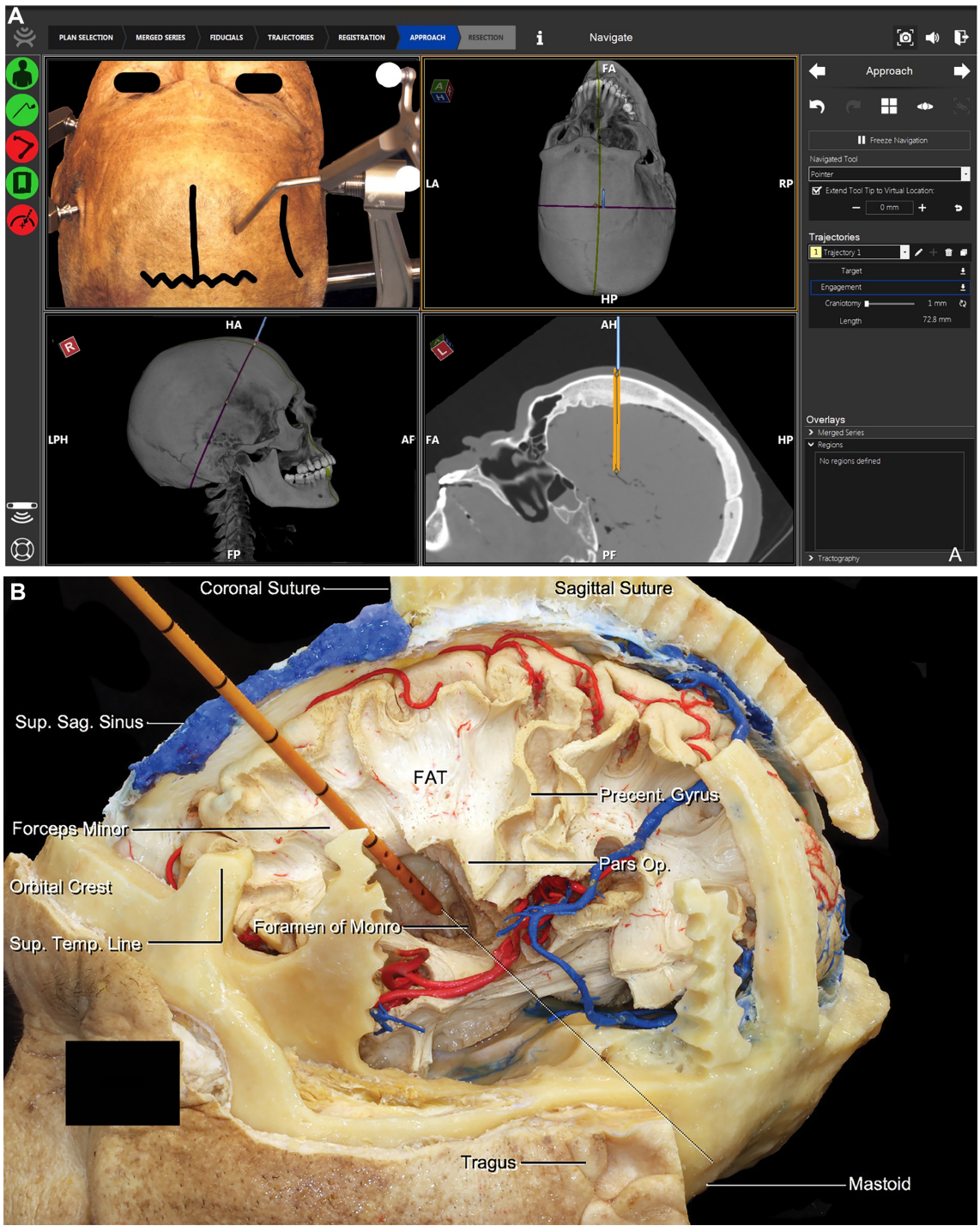

FIGURE 3. *Navigation guidance and anatomic correlation of the superior frontal sulcal entry point.* **A**, *Navigation tool was used to collocate the SFS parafascicular EP (x = 2.3 cm from the midline, y = 3.5 from the coronal suture) directed towards the frontal horn and then triangulating along a line bisecting the plane of the ipsilateral medial canthus and posterior of the mastoid tip.* **B**, *A ventricular catheter was positioned with the same EP and trajectory in an anatomic dissection, using the surface landmarks as a direction to the frontal horn. FAT was avoided and the forceps minor was traversed to reach the ventricle. FAT = frontal aslant tract; Op. = opercularis; Precent. = precentral; Sup. = superior; Sag. = sagittal; Sup. = superior; Temp. = temporal.*

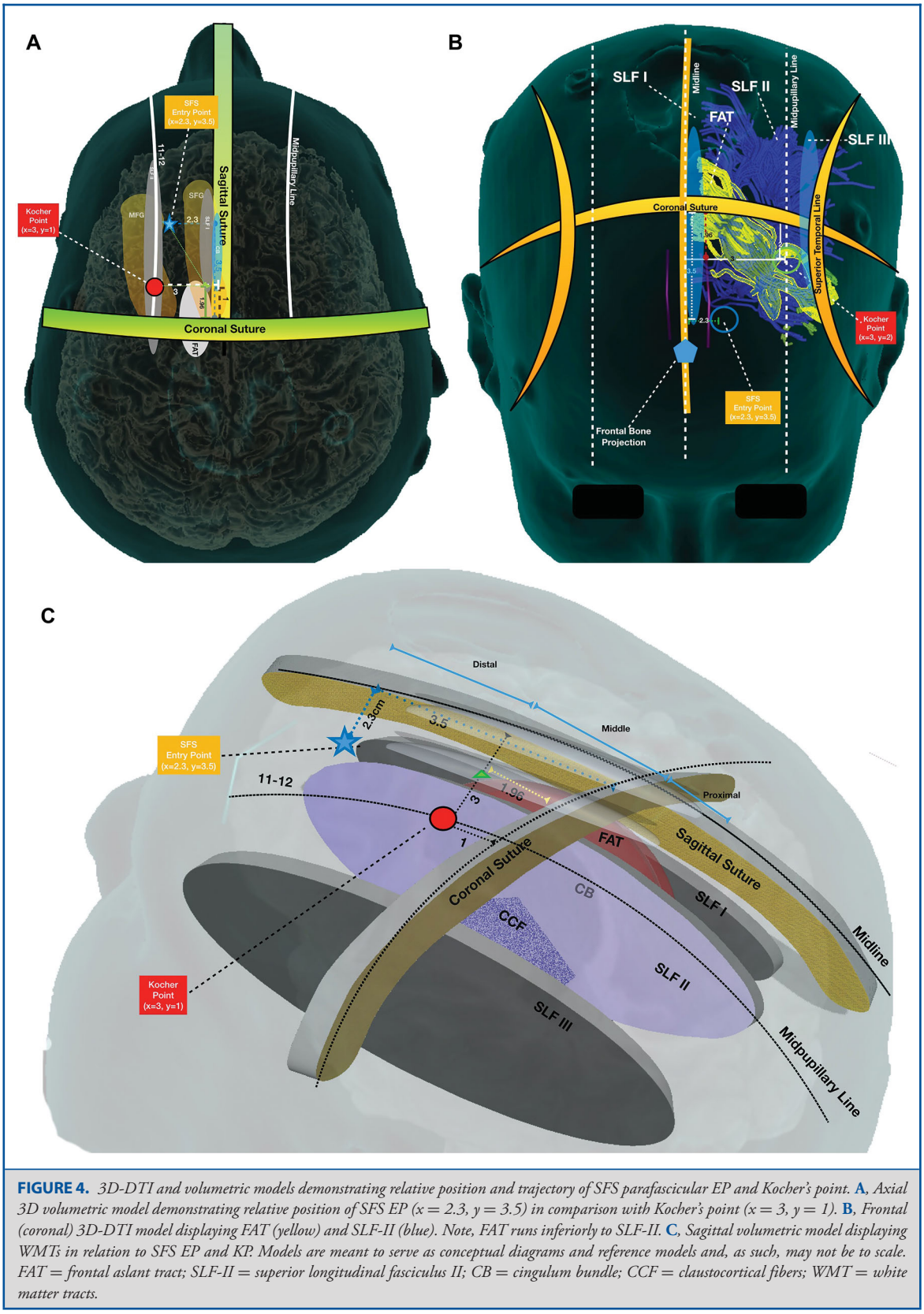

FIGURE 4. *3D-DTI and volumetric models demonstrating relative position and trajectory of SFS parafascicular EP and Kocher's point.* **A**, *Axial 3D volumetric model demonstrating relative position of SFS EP (x = 2.3, y = 3.5) in comparison with Kocher's point (x = 3, y = 1).* **B**, *Frontal (coronal) 3D-DTI model displaying FAT (yellow) and SLF-II (blue). Note, FAT runs inferiorly to SLF-II.* **C**, *Sagittal volumetric model displaying WMTs in relation to SFS EP and KP. Models are meant to serve as conceptual diagrams and reference models and, as such, may not be to scale. FAT = frontal aslant tract; SLF-II = superior longitudinal fasciculus II; CB = cingulum bundle; CCF = claustocortical fibers; WMT = white matter tracts.*

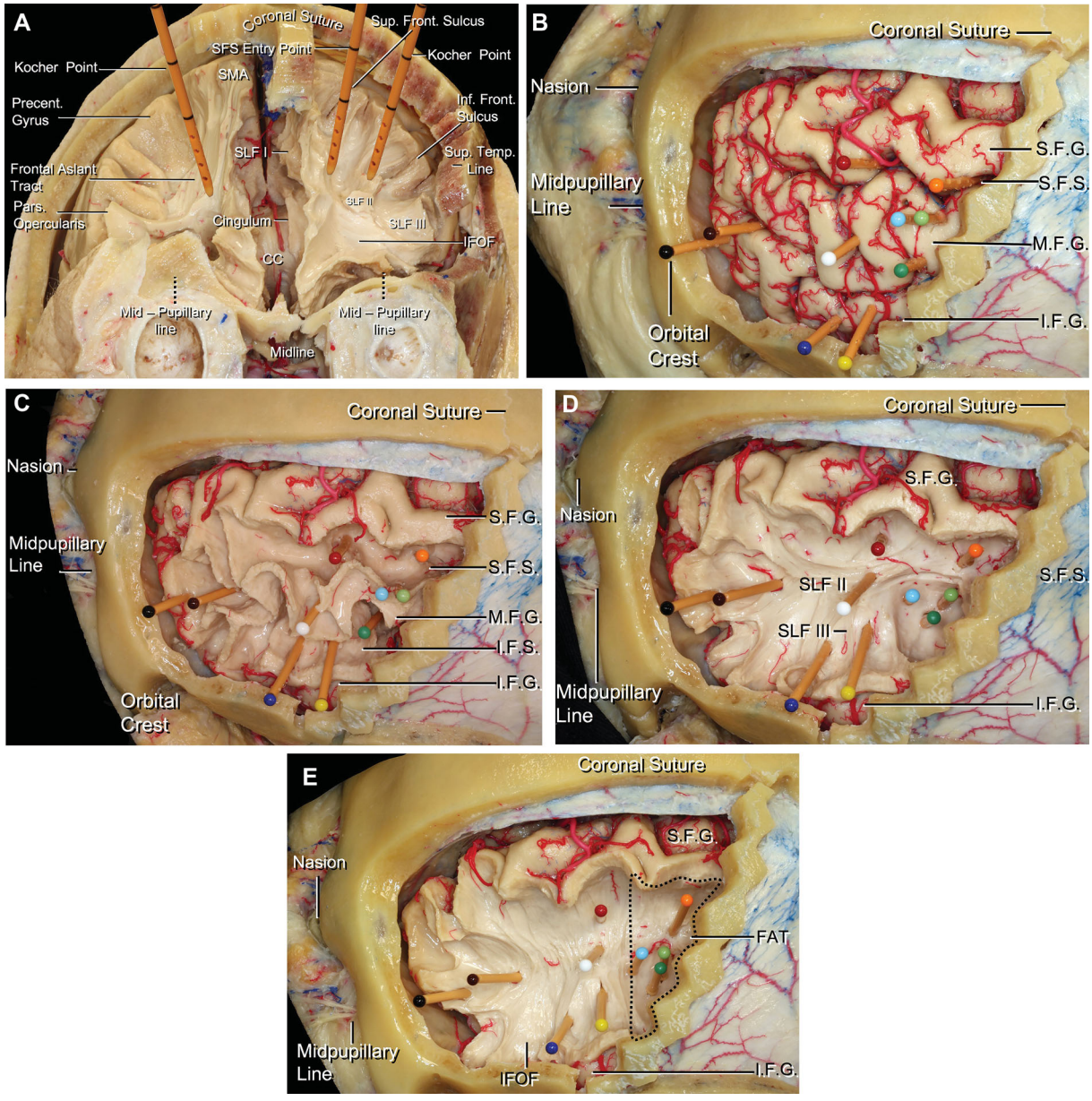

FIGURE 5. *Stepwise dissections showing relative WMT relationships with KP and major variant ventricular points.* **A**, *Coronal-facing dissection simulating catheter placement for both KP and SFS EP. KP trajectory directly interacts with SLF-II and IFOF.* **B**-**E**, *Stepwise WMT dissection displaying relative position of KP and several major variations, with each colored needle representing a different ventricular point. Explicitly,* **B** *represents initial gyral and sulcal anatomy, followed by progressive exposure of WMTs in* **C** *and* **D** *(revealing SLF-II and III), and* **E** *(revealing IFOF and FAT (represented by dotted region)). Ventricular points by color: light blue = Kocher (x = 3, y = 1 cm ant. to CS); green = Lewis et al[9] (x = 5 cm, y = 1 cm ant. to CS); pink = Abdou and Cohen[7] (x = MPL, y = 1 cm ant. to CS); blue = Rodziewicz et al[46] (x = 3-5 cm, y = 2 cm ant. to CS); orange = Zohdi and El Kheshin[48] (x = 3 cm, y = 1 cm ant. to KP (precoronal)); dark blue = Greenlee et al[51] (x = 7 cm, y = 8 cm above nasion); white = Mishra et al[54] (x = 4-5 cm, y = 4 cm ant. to CS); black = Delitala et al[34] (x-MPL, y = 1.5 cm above orbital rim); yellow = Rangel-Castilla et al[37] (x = 4 cm, y = 4.5 cm ant. to CS); and brown = Nasi et al[8] (x = MPL, y = 2.5-3 cm above eyebrow). Precent. Gyrus = precentral gyrus; SLF-I = superior longitudinal fasciculus I; SLF-II = superior longitudinal fasciculus II; SLF-III = superior longitudinal fasciculus III; SMA = supplementary motor area; CC = corpus callosum; Inf. Front. Sulcus = inferior frontal sulcus; Sup. Temp. Line = superior temporal line; IFOF = inferior fronto-occipital fasciculus; S.F.G. = superior frontal gyrus; S.F.S. = superior frontal sulcus; M.F.G. = middle frontal gyrus; I.F.G. = inferior frontal gyrus; I.F.S. = inferior grontal sulcus; FAT = frontal aslant tract; MPL = midpupillary line.*

TABLE 3. White Matter Tracts of the SFS Complex: Connectivity and Functional Role

	Cortical connectivity	Dominant hemisphere	Nondominant hemisphere
Lateral SFS segments			
U-fibers	SFG-MFG	Short association fibers connecting gyri at any point in cerebral cortex	Short association fibers connecting gyri at any point in cerebral cortex
Superior longitudinal fasciculus II	Angular gyrus – midpart of the middle frontal gyrus	Visual and oculomotor aspects of spatial function Spatial working memory Attention	
Inferofrontooccipital fasciculus	Frontal pole, orbito-fronto cortex, IFG, MFG, and SFG – planum temporal, SPL, and occipital cortex	Lexical-semantic processing, visual spatial processingReading, attention, and visual processing	Lexical-semantic processing
Coronal radiata – intervening segment			
Claustrocortical fibers *(crossing fiber)*	Claustrum to orbitofrontal areasPremotor areaSupplementary motor area	Executive function, cognitive controlExecutive function, cognitive controlSensory guidance of movement	Executive function, cognitive controlExecutive function, cognitive controlSensory guidance of movement
Thalamic prefrontal peduncle	Anterior, medial, the ventral posterior part of the medial, lateral dorsal and lateral posterior nuclei to areas in the prefrontal cortex included the SFG, MSFG, MFG, Ptri, Porp, LOG, and AOG	The function of the prefrontal cortex has been researched extensively and includes cognitive abilities, social emotion, executive functioning, motor control, and language	The function of the prefrontal cortex has been researched extensively and includes cognitive abilities, social emotion, executive functioning, and motor control
Frontopontine fibers	Premotor, prefrontal and dorsolateral prefrontal cortex (SFG and MFG) to the pontine nuclei	Motor function and connection to the cerebellum	Motor function and connection to the cerebellum
Frontal striatal tract	Pre-SMA and SMA proper to the anterior part of the caudate nucleus and putamen	Verbal fluency in speech; voluntary motor control	Voluntary motor control
Corona Radiata – intervening segment			
Corticospinal tract Corticobulbar tract	Motor area, premotor, supplementary area, motor cortex of the cingulum, and the postcentral gyrus to the spinal cord	Pyramidal motor system	Pyramidal motor system
Medial SFS segments			
Frontal aslant tract (FAT) *(crossing fiber)*	Pre-SMA and SMA proper –pars opercularis and pars triangularis	Speech initiation Verbal fluency	
Callosal fibers	Superior frontal gyrus – Superior frontal gyrus. Frontal callosal	Motor, sensory, and cognitive integration between cerebral hemispheres	Motor, sensory, and cognitive integration between cerebral hemispheres
Cingulum bundle	Temporal pole – rostral subcallosal area in the orbital frontal cortex	Executive function, decision-making, and emotion processing Execution of motor- and attention-related tasks Cognitive function	Executive function, decision-making, and emotion processing Execution of motor- and attention-related tasks Cognitive function
Superior longitudinal fasciculus I	Precuneus – pre-SMA and SMA proper	Regulation of higher aspects of motor function, initiation of motor activity, activation in resting state, integration of internally and externally driven information	Regulation of higher aspects of motor function, initiation of motor activity, activation in resting state, integration of internally and externally driven information

SFG = superior frontal gyrus, IFG = inferior frontal gyrus, MFG = middle frontal gyrus, SPL = superior parietal lobule, MSFG = medial superior frontal gyrus, Ptri = pars triangularis, Porp = pars opercularis, AOG = anterior orbital gyrus, LOG = lateral orbital gyrus, SMA = supplementary motor area.

anterior-posterior plane within 1.96 cm of CS, directly placed FAT at risk.

For the convenience of the reader, Table 3 describes the cortical connectivity and presumed functional importance of the WMTs of the SFS subcortical region.

DISCUSSION

Kocher in 1894[1] developed a craniometer as the first method of neurosurgical navigation culminating in 2 "coordinate" points to consistently access the ventricles.[11,13] KP is situated

approximately 1 cm anterior to CS, laterally marked by the midpupillary line (3 cm from midline) and 11 cm posterior from the glabella. The lateral distance was explicitly determined to avoid bridging veins. The coordinates target the FM of the ipsilateral lateral ventricle, with the catheter trajectory angled towards the ipsilateral medial canthus.

Kocher's Point defined over a century ago, representing the most commonly used EP to access the frontal horn, was based exclusively on osseous landmarks and venous considerations. Multiple variations have been proposed based on an evolving understanding of vascular and cortical anatomy.[18]

Over the past 2 decades, there has been an exponential evolution of neural imaging, such as the Human Connectome project,[50,51] increasing the conspicuity of the subcortical architecture and leading to the current "white matter era." Recently, advancements of MR-DTI are being coupled with the increasing awareness of the functional significance of the subcortical WMTs, particularly with respect to executive and neurocognitive function.[13,21,50-52] This convergence provided us an opportunity to further refine and inform the optimal trajectory to the frontal horn. This is of greater significance in an era of corridor surgery; particularly, as there is a suggestion that the incremental risk to underlying WMTs may be a direct function of the diameter and form of the corridor.[49] Intuitively, a 20-mm tubular corridor in comparison to a 4-mm catheter-based corridor has the potential of a more significant impact on traversed WMTs, particularly if an unintended complication such as a hemorrhage occurs.

In the first instance, this report documents, through detailed anatomic dissections and radiological analysis, the relative anatomic risk of KP and its variants to underlying WMTs. Explicitly, when subjecting KP and variations to a WMT traversed anatomic analysis, all EPs reported to date pose significant anatomic risk.

Potential Anatomic Impact of KP

In the case of KP (y = 1 cm, x = 3 cm), entering 1 cm anterior to CS directly places the anterior portion of FAT as well as the CCF of the intervening segment immediately in the path of the trajectory. Furthermore, in an effort to avoid bridging veins, moving the coronal entry 3 cm lateral to SSS places SLF-II directly in the path of the KP trajectory (Figures 4 and 5).

Next, when the same anatomic WMT analysis is systematically applied to each variation, progressive WMTs are at "anatomic risk." The further lateral the EP, the more acute, and thereby, less parafascicular, ie, less parallel and more orthogonal, the trajectory required to access the frontal horn. This acutely angled trajectory traverses the tracts en route to the frontal horn at a steeper angle, increasing potential anatomic transection risk. With respect to FAT, it is very difficult to develop a true parafascicular trajectory to FAT given that it is actually a crossing fiber of the SFS-intervening segment. Therefore, it can only be avoided by entering in the SFS-DD devoid of FAT and not the SFS-MD.

Purpose-Built SFSP-EP and Trajectory to the Frontal Horn

With an expressed intent to mitigate potential subcortical anatomic impact of the frontal horn trajectory, we purpose-built and designed an optimized corridor. Several considerations were incorporated into the algorithm. First, to avoid inadvertent effect on the cortical structures, we selected a sulcal, as opposed to a gyral EP, particularly when anything other than a ventricular catheter is used, ie, through-channel endoscopy or tubular retractor. Next, given the x-axis (lateral) location of the SFS (x = 2.3), specifically less than 3 cm in the coronal plane from the SSS, naturally led us to the SFS, as opposed to the IFS to avoid the lateral segment subcortical WMTs. Finally, based on our anatomic and radiological data, notably the position of the FAT, the ideal EP in the y-axis (anterior-posterior) must by definition be greater than 3.5 cm anterior to the CS, thus placing it in the distal SFS division. Consequently, the KM-EP in the y-axis must engage greater than 3.5 cm anterior to CS and 2.3 cm in the y-axis, yielding coordinates of x = 2.3 cm and y ≥ 3.5 cm. Given the orthogonal nature of the subcortical framework, it is impossible to access the frontal horn without placing some WMTs at risk. Using a 13.5-mm tubular retractor (15.5 mm outer diameter) via the KM-EP, we document a 9 mm disruption of the forceps minor, which we believe to be the most clinically silent of all of possible WMTs traversed.

Limitations

We would like the reader to consider the preceeding discussion in the context of significant limitations of this report, and therefore, present them prior:

(a) Correlation: first and foremost, a significant assumption is being made: explicitly, anatomic risk equals clinical risk, ie, disruption of subcortical anatomic pathways directly and proportionally leads to correlative clinical deficits. To date, despite emerging studies in the functional literature, particularly identification of ablative and stimulatory novel targets increasingly being reported, there is an absence of robust data to substantiate the correlation.
(b) Sparsity of data: there is a sparsity of data correlating anatomic with clinical neurocognitive pathways.[13]
(c) Physics: there are emerging limited studies suggesting transsulcal parafascicular surgery is clinically safe; however, parafascicular trajectories, although intuitively obvious, have not been mathematically established. Comparative and basic physics studies are lacking. Analogously, the premise that larger diameter corridors and increased volumes, including complications, lead to greater WMT risk have not been systematically proven, other than a few limited reports,[50] ie, the maximal volume leading to injury in a given population has not been established and will be subject to individual variation.

(d) Variation, plasticity, and measurements: significant variation exists, and in fact, there may be plasticity/reduplication in neurocognitive and executive function between individuals when coupled with poor sensitivities and specificities of current assay, thus making reproducible assessment difficult.

(e) WMT fiber segmentation: there may lie an inherent operator variability in fiber dissection technique when attempting to precisely segmenting and identifying white matter fiber bundles. This can be due to variety of factors, including operator experience and ability, a priori anatomic knowledge, and, possibly more importantly, the inherent relative position and orientation of WMTs relative to each other (ie, "kissing" fibers). For example, accurate delineation of fine fibers, such as FAT, SLF-I, and SLF-II, and noting their relative position, measurement, and osseous and vascular relationships may be difficult and limited in certain specimens but can be performed with careful and systematic dissection. In addition, IFOF can, in some cases, merge with CCF or fibers of the external and internal capsule; this may limit the ability to clearly delineate all fibers of the IFOF. Similar variability can exist with currently available radiological segmentation algorithms. Explicitly, a primary limitation with respect to variability in voxel seeding, in that computer-generated DTI models cannot be considered equivalent to physical axons in size, length, and direction. In addition, algorithm-dependent variability can exist in detecting crossing, "kissing," sharply angulated or intermingled tracts, which may make tract segmentation difficult.

It is important for the reader to be aware of all of the limitations above prior to interpreting any of the data, recommendations, or concepts noted in this report.

CONCLUSION

Founded on anatomic and 3D-MRI-DTI renderings, we propose a purpose-built ventricular access coordinate, the KM-EP ($x = 2.3$ cm, $y \geq 3.5$ cm). These coordinates are founded on the WMT subcortical framework, most critically FAT, SLF-II/III, and IFOF. Our EP is located in the distal division of the SFS, a minimum of 3.5 cm anterior to CS, 2.3 cm lateral to SSS, and along a parafascicular trajectory paralleling corona radiata. Emergently and in the absence CASN, the KM-EP can be approximated by entering 3.5 cm anterior to CS (in front of FAT), bisecting the distance between the midline (cingulum bundle, SLF-I) and midpupillary line (SLF-II) and then triangulating on a line bisecting the plane of the ipsilateral medial canthus and posterior tip of the mastoid (as opposed to the tragus in KP).

We believe this cosmetic consideration is justified by the anatomic WMT preservation. In the final analysis, in contrast to all other EPs reported to date, we have not found an anatomic or clinical reason to not use KM-EP while we await the prospective neurocognitive clinical studies.

Disclosures

This research is supported by an award to the Aurora Research Institute by the Vince Lombardi Cancer Foundation. This work was supported by donations from NICO Corp., Carl Zeiss, Stryker Corporation, and Karl Storz SE & Co/Karl Storz Endoscopy America Inc. The authors have no personal, financial, or institutional interest in any of the drugs, materials, or devices described in this article. Dr Kassam reports involvement as a consultant to Synaptive Medical, KLS Martin Medical, Stryker Corporation, and the Medtronic Advisory Board and as a founder and CEO of Neeka Health LLC.

REFERENCES

1. Hildebrandt G, Surbeck W, Stienen MN. Emil Theodor Kocher: the first Swiss neurosurgeon. *Acta Neurochir*. 2012;154(6):1105-1115; discussion 1115.
2. Dandy WE. Ventriculography following the injection of air into the cerebral ventricles. *Ann Surg*. 1918;68(1):5-11.
3. Hyun SJ, Suk JS, Kwon JT, Kim YB. Novel entry point for intraoperative ventricular puncture during the transsylvian approach. *Acta Neurochir (Wien)*. 2007;149(10):1049-1051; discussion 1051.
4. Kaufmann GE, Clark K. Emergency frontal twist drill ventriculostomy. *J Neurosurg*. 1970;33(2):226-227.
5. Menovsky T, De Vries J, Wurzer JAL, Grotenhuis JA. Intraoperative ventricular puncture during supraorbital craniotomy via an eyebrow incision. *J Neurosurg*. 2006;105(3):485-486.
6. Paine JT, Batjer HH, Samson D. Intraoperative ventricular puncture. *Neurosurgery*. 1988;22(6P1-P2):1107-1109.
7. Abdou MS, Cohen AR. Endoscopic treatment of colloid cysts of the third ventricle. *J Neurosurg*. 1998;89(6):1062-1068.
8. Nasi D, Iaccarino C, Romano A. Anterior trans-frontal endoscopic resection of third-ventricle colloid cyst: how I do it. *Acta Neurochir*. 2017;159(6):1049-1052.
9. Lewis AI, Crone KR, Taha J, van Loveren HR, Yeh HS, Tew JM. Surgical resection of third ventricle colloid cysts. *J Neurosurg*. 1994;81(2):174-178.
10. Kim D, Son W, Park J. Guiding protractor for accurate freehand placement of ventricular catheter in ventriculoperitoneal shunting. *Acta Neurochir*. 2015;157(4):699-702.
11. Park J, Hamm I-S. Revision of Paine's technique for intraoperative ventricular puncture. *Surg Neurol*. 2008;70(5):503-508; discussion 508.
12. Rosenbaum BP, Vadera S, Kelly ML, Kshettry VR, Weil RJ. Ventriculostomy: Frequency, length of stay and in-hospital mortality in the United States of America, 1988–2010. *J Clin Neurosci*. 2014;21(4):623-632.
13. Srinivasan VM, O'Neill BR, Jho D, Whiting DM, Oh MY. The history of external ventricular drainage. *J Neurosurg*. 2014;120(1):228-236.
14. Toma AK, Camp S, Watkins LD, Grieve J, Kitchen ND. External ventricular drain insertion accuracy: is there a need for change in practice? *Neurosurgery*. 2009;65(6):1197-1201; discussion 1200-1201.
15. Rehman T, Rehman A, Ali R, et al. A radiographic analysis of ventricular trajectories. *World Neurosurg*. 2013;80(1-2):173-178.
16. Wilson TJ, Stetler WR, Al-Holou WN, Sullivan SE. Comparison of the accuracy of ventricular catheter placement using freehand placement, ultrasonic guidance, and stereotactic neuronavigation. *J Neurosurg*. 2013;119(1):66-70.
17. Wilson DA, Fusco DJ, Wait SD, Nakaji P. Endoscopic resection of colloid cysts: use of a dual-instrument technique and an anterolateral approach. *World Neurosurg*. 2013;80(5):576-583.
18. Chakravarthi SS, Kassam AB, Fukui MB, et al. Awake surgical management of third ventricular tumors: a preliminary safety, feasibility, and clinical applications study. *Oper Neurosurg*. 2019;17(2):208-226.
19. Jennings JE, Kassam AB, Fukui MB, et al. The surgical white matter chassis: a practical 3-dimensional atlas for planning subcortical surgical trajectories. *Oper Neurosurg*. 2018;14(5):469-482.
20. McLaughlin N, Prevedello DM, Engh J, Kelly DF, Kassam AB. Endoneurosurgical resection of intraventricular and intraparenchymal lesions using the port technique. *World Neurosurg*. 2013;79(2):S18.e1-S18.e8.
21. Amenta PS, Dumont AS, Medel R. Resection of a left posterolateral thalamic cavernoma with the Nico BrainPath sheath: case report, technical note, and review of the literature. *Interdiscip Neurosurg*. 2016;5:12-17.
22. Labib MA, Shah M, Kassam AB, et al. The safety and feasibility of image-guided brainpath-mediated transsulcul hematoma evacuation: a multicenter study. *Neurosurgery*. 2016;80(4):1.

23. Eliyas JK, Glynn R, Kulwin CG, et al. Minimally invasive transsulcal resection of intraventricular and periventricular lesions through a tubular retractor system: multicentric experience and results. *World Neurosurg*. 2016;90:556-564.
24. Day JD. Transsulcal parafascicular surgery using brain path® for subcortical lesions. *Neurosurgery*. 2017;64(CN_Suppl_1):151-156.
25. Ritsma B, Kassam A, Dowlatshahi D, Nguyen T, Stotts G. Minimally invasive subcortical parafascicular transsulcal access for clot evacuation (mi space) for intracerebral hemorrhage. *Case Rep Neurol Med*. 2014;2014:1-4.
26. Eliyas JK, Bailes J. Nt-14 early experience with trans-sulcal parafascicular exoscopic resection of supratentorial brain tumors. *Neuro-oncol*. 2014;16(Suppl 5):v161.
27. Mandonnet E, Martino J, Sarubbo S, et al. Neuronavigated fiber dissection with pial preservation: laboratory model to simulate opercular approaches to insular tumors. *World Neurosurg*. 2017;98:239-242.
28. Ko K, Webster JM. Holographic imaging of human brain preparations–a step toward virtual medicine. *Surg Neurol*. 1995;44(5):428-432.
29. Jakola AS, Reinertsen I, Selbekk T, et al. Three-dimensional ultrasound-guided placement of ventricular catheters. *World Neurosurg*. 2014;82(3-4):536.e5-536.e9.
30. Cabbell KL, Ross DA. Stereotactic microsurgical craniotomy for the treatment of third ventricular colloid cysts. *Neurosurgery*. 1996;38(2):301-307.
31. Krötz M, Linsenmaier U, Kanz KG, Pfeifer KJ, Mutschler W, Reiser M. Evaluation of minimally invasive percutaneous CT-controlled ventriculostomy in patients with severe head trauma. *Eur Radiol*. 2004;14(2):227-233.
32. Harris AE, Hadjipanayis CG, Lunsford LD, Lunsford AK, Kassam AB. Microsurgical removal of intraventricular lesions using endoscopic visualization and stereotactic guidance. *Neurosurgery*. 2008;62(Suppl 2):622-629.
33. Engh JA, Lunsford LD, Amin DV, et al. Stereotactically guided endoscopic port surgery for intraventricular tumor and colloid cyst resection. *Neurosurgery*. 2010;67(3 Suppl operative):ons198-204; discussion ons204-205.
34. Delitala A, Brunori A, Russo N. Supraorbital endoscopic approach to colloid cysts. *Neurosurgery*. 2011;69(2 Suppl Operative):ons176-182; discussion ons182-183.
35. Thomale UW, Knitter T, Schaumann A, et al. Smartphone-assisted guide for the placement of ventricular catheters. *Childs Nerv Syst*. 2013;29(1):131-139.
36. Cohen-Gadol AA. Minitubular transcortical microsurgical approach for gross total resection of third ventricular colloid cysts: technique and assessment. *World Neurosurg*. 2013;79(1):207.e7-207.e10.
37. Rangel-Castilla L, Chen F, Choi L, Clark JC, Nakaji P. Endoscopic approach to colloid cyst: what is the optimal entry point and trajectory? *J Neurosurg*. 2014;121(4):790-796.
38. Eichberg DG, Buttrick SS, Sharaf JM, et al. Use of Tubular Retractor for Resection of Colloid Cysts: Single Surgeon Experience and Review of the Literature. *Oper Neurosurg*. 2019;16(5):571-579.
39. Tillmanns H. Some points about puncture of the brain. *Lancet North Am Ed*. 1908;172(4443):1212-1213.
40. Madrazo Navarro I, Garcia Renteria JA, Rosas Peralta VH, Dei Castilli MA. Transorbital ventricular puncture for emergency ventricular decompression. *J Neurosurg*. 1981;54(2):273-274.
41. Ghajar JB. A guide for ventricular catheter placement. *J Neurosurg*. 1985; 63(6): 985-986.
42. Decq P, Le Guerinel C, Brugières P, et al. Endoscopic management of colloid cysts. *Neurosurgery*. 1998;42(6):1288-1294; discussion 1294-1296.
43. King WA, Ullman JS, Frazee JG, Post KD, Bergsneider M. Endoscopic resection of colloid cysts: surgical considerations using the rigid endoscope. *Neurosurgery*. 1999;44(5):1103-1109; discussion 1109-1111.
44. Teo C. Complete endoscopic removal of colloid cysts: issues of safety and efficacy. *Neurosurg Focus*. 1999;6(4):e9.
45. Longatti P, Martinuzzi A, Moro M, Fiorindi A, Carteri A. Endoscopic treatment of colloid cysts of the third ventricle: 9 consecutive cases. *Minim Invasive Neurosurg*. 2000;43(3):118-123.
46. Rodziewicz GS, Smith MV, Hodge CJ. Endoscopic colloid cyst surgery. *Neurosurgery*. 2000;46(3):655-662; discussion 660-662.
47. O'Leary ST, Kole MK, Hoover DA, Hysell SE, Thomas A, Shaffrey CI. Efficacy of the Ghajar Guide revisited: a prospective study. *J Neurosurg*. 2000;92(5):801-803.
48. Zohdi A, El Kheshin S. Endoscopic approach to colloid cysts. *Minim Invasive Neurosurg*. 2006;49(5):263-268.
49. Acerbi F, Rampini P, Egidi M, Locatelli M, Borsa S, Gaini SM. Endoscopic treatment of colloid cysts of the third ventricle: long-term results in a series of 6 consecutive cases. *J Neurosurg Sci*. 2007;51(2):53-60.
50. Levine NB, Miller MN, Crone KR. Endoscopic resection of colloid cysts: indications, technique, and results during a 13-year period. *Minim Invasive Neurosurg*. 2007;50(6):313-317.
51. Greenlee JDW, Teo C, Ghahreman A, Kwok B. Purely endoscopic resection of colloid cysts. *Neurosurgery*. 2008;62(3 Suppl 1):51-55; discussion 55-56.
52. Kakarla UK, Kim LJ, Chang SW, Theodore N, Spetzler RF. Safety and accuracy of bedside external ventricular drain placement. *Neurosurgery*. 2008;63(1 Suppl 1):ONS162-166; discussion ONS166-167.
53. Ehtisham A, Taylor S, Bayless L, Klein MW, Janzen JM. Placement of external ventricular drains and intracranial pressure monitors by neurointensivists. *Neurocrit Care*. 2009;10(2):241-247.
54. Mishra S, Chandra PS, Suri A, Rajender K, Sharma BS, Mahapatra AK. Endoscopic management of third ventricular colloid cysts: eight years' institutional experience and description of a new technique. *Neurol India*. 2010;58(3):412-417.
55. Boogaarts H, El-Kheshin S, Grotenhuis J. Endoscopic colloid cyst resection: technical note. *Minim Invasive Neurosurg*. 2011;54(2):95-97.
56. Hsieh C-T, Chen G-J, Ma H-I, et al. The misplacement of external ventricular drain by freehand method in emergent neurosurgery. *Acta Neurol Belg*. 2011;111(1):22-28.
57. Yamada SM, Yamada S, Goto Y, et al. A simple and consistent technique for ventricular catheter insertion using a tripod. *Clin Neurol Neurosurg*. 2012;114(6):622-626.
58. Abdoh MG, Bekaert O, Hodel J, et al. Accuracy of external ventricular drainage catheter placement. *Acta Neurochir*. 2012;154(1):153-159.
59. Kim JH, Kang HI. Intraoperative ventriculostomy using k point in surgical management of aneurysmal subarachnoid hemorrhage. *World Neurosurg*. 2019;122:e248-e252.
60. Aref M, Martyniuk A, Nath S, et al. Endoscopic third ventriculostomy: outcome analysis of an anterior entry point. *World Neurosurg*. 2017;104:554-559.

Acknowledgments

We would like to thank Nico Corporation, Carl Zeiss, Stryker Medical, and Karl Storz for their donations that made our research possible in the Neuroanatomy Laboratory.

COMMENT

In this Part II of the article, the authors revisit the classical Kocher's point and propose a more anterior and medial frontal entry point to reach the frontal horn based in anatomical findings pertinent to the underlying fiber tracts. Our considerations and concerns related the limitations of both fiber dissection technique and DTI findings are addressed in our comments of Part I of this study.

Despite lack of direct evidences of measured neurological impairments related with the already long neurosurgical experience with the Kocher's point, we do agree that a more anterior frontal approach to the ventricular cavity might be less hazardous specially when larger diameter tubular retractors are introduced for parafascicular procedures, particularly by potentially sparing SMA-frontal opercular connecting fibers that might be functionally important especially in the dominant hemispheres, as proposed in this elegant article.

Considering the classical and well established relationship of the midline portion of the Coronal suture with the foramina of Monro along a coronal plane, the Kocher's point which is located 1 centimeter anterior to the coronal suture is systematically vertically related with the anterior horn of the ventricle, and the point 3.5 centimeters anterior to the coronal suture here suggested hence requires a more inclined route to reach the ventricle.

Guilherme C. Ribas
São Paulo, Brazil